

# National Seismic Hazard Maps of Japan

Hiroyuki Fujiwara\*, Shinichi Kawai, Shin Aoi, Nobuyuki Morikawa, Shigeki Senna,  
Kyoko Kobayashi, Toru Ishii, Toshihiko Okumura and Yuzuru Hayakawa

National Research Institute for Earth Science and Disaster Prevention, Japan

## Abstract

The Headquarters for Earthquake Research Promotion (HERP) of Japan published the national seismic hazard maps of Japan in March 2005, at the initiation of the earthquake research committee of Japan (ERCJ), on the basis of a long-term evaluation of seismic activity and a strong-motion evaluation. Meanwhile, the National Research Institute for Earth Science and Disaster Prevention (NIED) also promoted the special research project named National Seismic Hazard Mapping Project of Japan to support preparation of the seismic hazard maps. Under the guidance of ERCJ, we carried out a study of the hazard maps. There are 2 types of hazard map: one is a probabilistic seismic hazard map (PSHM), which shows the relation between seismic intensity value and its probability of exceedance within a certain time; the other is a scenario earthquake shaking map (SESM). For the PSHM, we used an empirical attenuation formula for strong-motion, which followed seismic activity modeling by ERCJ. Both peak velocity on the engineering bedrock ( $V_s=400$  m/s) and on the ground surface are evaluated for sites with a spacing of approximately 1 km. The potential JMA seismic intensities on the ground surface are also evaluated using an empirical formula. For the SESMs, based on source modeling for strong-motion evaluation, we adopted a hybrid method to simulate waveforms on the engineering bedrock and peak ground velocity. For this project, we developed an open web system to provide information interactively and retrievably, and named the system Japan Seismic Hazard Information Station, J-SHIS (<http://www.j-shis.bosai.go.jp>). We aimed to distribute the process of uncertainty evaluation, and to meet multi-purpose needs in engineering fields. The information provided by J-SHIS includes not only the hazard map results, but also various information required in the processes of making the hazard maps, such as data on seismic activity, source models, and underground structure.

**Key words:** Seismic Hazard Map, Probability, Shaking map, J-SHIS

## 1. Introduction

The great Hanshin-Awaji earthquake, which occurred on January 17, 1995, killed more than 6,400 persons. Following the lessons learned from this disaster, A Special Act of Earthquake Disaster Management was enacted in July 1995 to promote a comprehensive national policy on earthquake disaster prevention. The Headquarters for Earthquake Research Promotion (HERP) was established in accordance with this act. In April 1999, HERP issued 'On Promotion of Earthquake Research-Comprehensive and Fundamental Measures for Promotion of Observation, Measurement and Research on Earthquakes'. In this article, HERP concluded that preparation of 'National Seis-

mic Hazard Maps of Japan' should be promoted as a major subject of earthquake research. The National Research Institute for Earth Science and Disaster Prevention (NIED) then started a special project in April 2001 named 'National Seismic Hazard Mapping Project of Japan' to support preparation of seismic hazard maps. After 4 years of study, in March 2005 HERP published the 'National Seismic Hazard Maps of Japan,' which was initiated by the earthquake research committee of Japan (ERCJ) on the basis of a long-term evaluation of seismic activity and strong-motion evaluation.

Under the guidance of ERCJ, we carried out a hazard map study. There are 2 types of hazard map.

\* e-mail: fujiwara@bosai.go.jp (3-1, Tennodai, Tsukuba, Ibaraki, 305-0006, Japan)

One is a probabilistic seismic hazard map (PSHM), which shows the relation between seismic intensity value and its probability of exceedance within a certain time. The other is a scenario earthquake shaking map (SESM). For the PSHM, we used an empirical attenuation formula for strong-motion, which followed the seismic activity modeling carried out by ERCJ. Both peak velocity on the engineering bedrock ( $V_s=400$  m/s) and on the ground surface were evaluated for every site spaced approximately 1 km apart. The potential JMA seismic intensities on the ground surface were also evaluated using an empirical formula. For the SESMs, based on source modeling for a strong-motion evaluation, we adopted a hybrid method to simulate waveforms on the engineering bedrock layer and peak velocity on the ground surface.

For this project, we developed an open web system to provide information interactively and retrievably, and named it Japan Seismic Hazard Information Station, J-SHIS (<http://www.j-shis.bosai.go.jp/>). We aimed to distribute the process of uncertainty evaluation, and to meet multi-purpose needs in engineering fields. Information provided by J-SHIS includes not only the results of the hazard maps, but also various information required in the processes of making the hazard maps, such as data on seismic activity, source models, and underground structure.

## 2. Probabilistic seismic hazard map (PSHM)

### 2.1 Procedure of probabilistic seismic hazard analysis (PSHA)

Probability or annual rate of earthquake occurrence, and strong-motion levels for all possible earthquakes are evaluated for PSHMs. The PSHA procedure used in the Seismic Hazard Mapping Project is itemized below.

- (1) Following classification of earthquakes by ERCJ, we set up different mathematical models for characteristic seismic activities in Japan.
- (2) Occurrence probability is evaluated for each earthquake.
- (3) Probabilistic evaluation model of strong-motion level is selected for each earthquake.
- (4) Probability that the intensity measure of a strong-motion will exceed a certain level during a specified time is evaluated for each earthquake.
- (5) Considering contributions from all possible earth-

quakes, we evaluate the probability that the intensity measure of strong-motion will be exceeded during a specified time.

In procedure (3), we use an empirical attenuation relation (Si and Midorikawa, 1999) for an intensity measure of strong-motion.

The seismic hazard curve is a key concept, which gives the probability of exceeding a specific level from all possible earthquakes. Usually, a seismic hazard curve  $P(Y>y; t)$  is defined as

$$P(Y>y; t) = 1 - \prod_k \{1 - P_k(Y>y; t)\} \quad (1)$$

where  $P_k(Y>y; t)$  is the probability that a ground motion  $Y$  exceeds level  $y$  for the  $k$ -th earthquake within time  $t$ .

In the following sections we describe detailed procedures for calculating the seismic hazard curve in different source faults and using different probability models.

#### 2.1.1. PSHA for earthquakes with specified source faults

The occurrence probability of a potential earthquake with a specified source fault is evaluated using a) a renewal process such as a Brownian passage time distribution, or b) a Poissonian process.

The following procedure shows how to calculate probability  $P_k(Y>y; t)$  using time-dependent and time-independent probability models.

##### a) PSHA using time-dependent probability model

Assuming an independency of ground motion level for each earthquake, the probability  $P_k(Y>y; t)$  that the ground motion exceeds a specific level  $y$  is written as

$$P_k(Y>y; t) = 1 - \sum_{l=0}^{\infty} \{P(E_k^{[l]}; t) [1 - P(Y>y|E_k)]^l\} \quad (2)$$

where  $P(E_k^{[l]}; t)$  is a probability for  $l$  occurrences of the  $k$ -th earthquake over time  $t$  and  $P(Y>y|E_k)$  is a probability that a ground motion  $Y$  exceeds a level  $y$ , where the occurrence of the  $k$ -th earthquake is given.

$$P(Y>y|E_k) = \sum_i \sum_j P(Y>y|m_i, r_j) P_k(m_i) P_k(r_j|m_i) \quad (3)$$

where  $P_k(m_i)$  is a probability density function of the magnitude for the  $k$ -th earthquake;  $P_k(r_j|m_i)$  is the probability density function of the distance from the source to the site, and  $P(Y>y|m_i, r_j)$  is the conditional probability of exceedance while the occurrence of an

earthquake is given with magnitude  $m_i$  and distance  $r_j$ .

An attenuation relation is used to estimate mean ground motion  $\bar{Y}(m_i, r_j)$  as a function of magnitude and distance. Then  $P(Y > y | m_i, r_j)$  is written as

$$P(Y > y | m_i, r_j) = 1 - F_U\left(\frac{y}{\bar{Y}(m_i, r_j)}\right) \quad (4)$$

where  $U$  is a logarithmic normal distribution and  $F_U(u)$  is a cumulative function of  $U$ .

In the situation of a small occurrence-probability, where an earthquake reoccurs twice or more during time  $t$ , the probability is so small that it can be ignored; therefore, equation (2) can be written as

$$\begin{aligned} P_k(Y > y; t) &= P(E_k; t)P(Y > y | E_k) \\ &= P(E_k; t) \sum_i \sum_j P(Y > y | m_i, r_j) P_k(m_i) P_k(r_j | m_i) \end{aligned} \quad (5)$$

where  $P(E_k; t)$  is the occurrence probability of the  $k$ -th earthquake over time  $t$ . Then, the Brownian passage time distribution is adopted for evaluating  $P(E_k; t)$ .

b) PSHA using time-independent probability model

Assuming a Poissonian model, the probability  $P(Y > y; t)$  that a ground motion  $Y$  exceeds a specific level  $y$  over time  $t$  for the  $k$ -th earthquake, is given by

$$P_k(Y > y; t) = 1 - \exp\{-\nu_k(Y > y) \cdot t\} \quad (6)$$

where  $\nu_k(Y > y)$  is an annual rate exceeding a specific shaking level  $y$  for the  $k$ -th earthquake, and it can be written as

$$\begin{aligned} \nu_k(Y > y) &= \nu(E_k)P(Y > y | E_k) \\ &= \nu(E_k) \sum_i \sum_j P(Y > y | m_i, r_j) P_k(m_i) P_k(r_j | m_i) \end{aligned} \quad (7)$$

where  $\nu(E_k)$  is the mean annual rate of the  $k$ -th earthquake.

### 2.1.2. PSHA for earthquakes with non-specified source faults

In the case of a seismic hazard evaluation for earthquakes with non-specified source faults, the probability of earthquake occurrence can be modeled as a Poissonian process. The probability  $P(Y > y; t)$ , of a ground motion  $Y$  exceeding a specific level  $y$  over time  $t$ , is given by

$$P(Y > y; t) = 1 - \exp(-\nu(Y > y) \cdot t) \quad (8)$$

where  $\nu(Y > y)$  is the annual rate exceeding shaking level  $y$ , and it can also be written as

$$\begin{aligned} \nu(Y > y) &= \sum_k \nu(E_k)P(Y > y | E_k) \\ &= \sum_k \nu(E_k) \sum_i \sum_j P(Y > y | m_i, r_j) P_k(m_i) P_k(r_j | m_i) \end{aligned} \quad (9)$$

where  $\nu(E_k)$  is the mean annual rate in the  $k$ -th source area,  $P(Y > y | E_k)$  is the conditional probability that the ground motion exceeds level  $y$  given the occurrence of an earthquake in the  $k$ -th area.  $P_k(m_i)$  is the probability density function of magnitude for earthquakes in the  $k$ -th area;  $P_k(r_j | m_i)$  is the probability density function of distance to the site; and,  $P(Y > y | m_i, r_j)$  is the conditional probability of exceedance while the occurrence of an earthquake is given for magnitude  $m_i$  and distance  $r_j$ .

The probability density function of magnitude  $P(m_i)$  is derived from the Gutenberg-Richter relation. We set the maximum and minimum magnitudes,  $m_u$  and  $m_l$ , for each area, respectively. Then, the number of earthquakes classified by  $m_u$  and  $m_l$  is given by

$$N(m_l \leq M \leq m_u) = N(M \geq m_l) - N(M \geq m_u) \quad (10)$$

$$N(m_l \leq M \leq m) = N(M \geq m_l) - N(M \geq m) \quad (11)$$

Using the Gutenberg-Richter relation,

$$N(M \geq m) = 10^{a-bm} \quad (12)$$

the distribution function of magnitude is given by

$$\begin{aligned} F_M(m) &= P(M \leq m) \\ &= \frac{N(M \geq m_l) - N(M \geq m)}{N(M \geq m_l) - N(M \geq m_u)} \\ &= \frac{1 - 10^{-b(m-m_l)}}{1 - 10^{-b(m_u-m_l)}} \\ &= \frac{1 - \exp(-b \ln 10 (m - m_l))}{1 - \exp(-b \ln 10 (m_u - m_l))} \end{aligned} \quad (13)$$

Then, probability  $P_k(m_i)$  is written as

$$P(m_i) = P(m_1 \leq m_i \leq m_2) = F_M(m_2) - F_M(m_1) \quad (14)$$

where we put

$$m_i - \Delta m / 2 = m_1 \leq m_i < m_2 = m_i + \Delta m / 2.$$

## 2.2 Examples of PSHM

Using the PSHA procedure mentioned in 2.1, followed the seismic activity modeling by ERCJ, we produced PSHMs throughout Japan.

At each PSHM, peak velocity on the engineering bedrock ( $V_s = 400$  m/s) is first evaluated based on contributions by the empirical attenuation formula (Si and Midorikawa, 1999). Then, an amplification

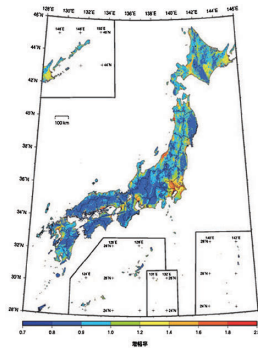


Fig. 1. A distribution of amplification factor generated by shallow surface layer based on Digital Nation Land Information based on geological data and geomorphological data.

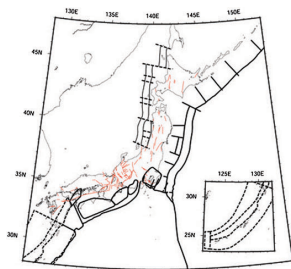


Fig. 2. Distributions for subduction zones, and 98 major faults where earthquake occurrence probabilities are evaluated by ERCJ.

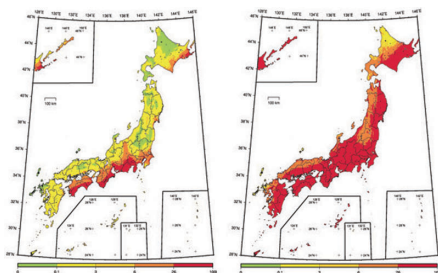


Fig. 3. The probability distributions in a color scale where seismic intensity exceeds (a) the JMA scale 6-, and (b) the JMA scale 5-, during the 30 years starting from January. 2005.

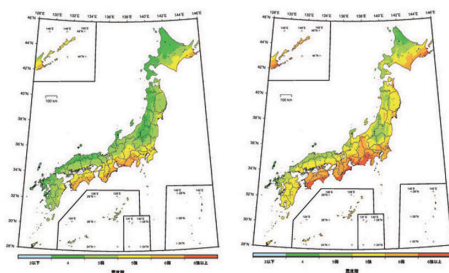


Fig. 4. JMA seismic intensity in a color scale corresponding to the exceedance probability of (a) 39%, and (b) 5%, during the 50 years starting from January 2005.

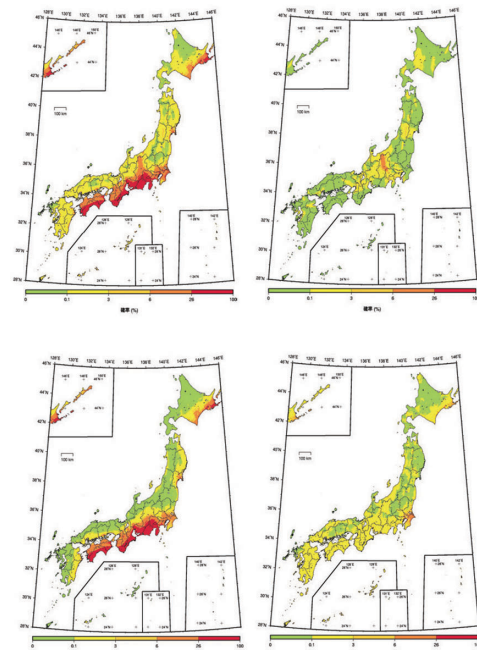


Fig. 5. The probability distributions in a color scale where seismic intensity exceeds the JMA scale 6- during the 30 years from January 2005. The PSHM (a) considers all contributions from all earthquakes, and is reprinted from Figure 3 (a) for comparison: the breakdown cases only consider contributions from (b) subduction zone earthquakes, (c) major 98 faults earthquakes, and (d) other earthquakes exclusive the cases (b) and (c).

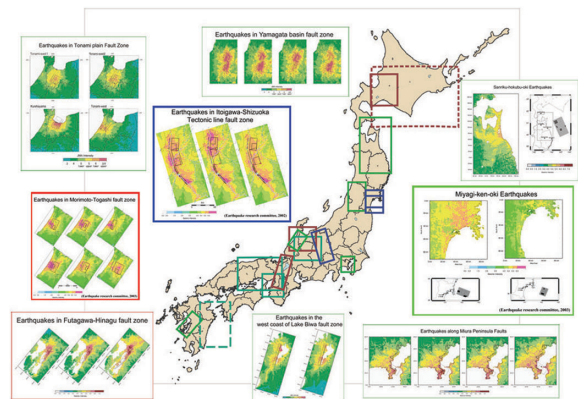


Fig. 6. SESMs were carried out for the fault zones with detailed investigation information. The colors stand for JMA intensities from 3 in green to 6+ or 7 in red.

factor dependent on surface geological sedimentary rocks, as shown in Figure 1, is used to obtain peak ground motions for the sites at spaces of approximately 1 km. JMA seismic intensities on the ground surface are also evaluated using an empirical formula (Midorikawa *et al.*, 1999).

Figure 2 shows distributions for subduction zones, and 98 major faults where earthquake occurrence probabilities were evaluated by ERCJ.

Figure 3 gives 2 PSHM examples for all of Japan (ERCJ 2005). The maps show probabilities that seismic intensity exceeds (a) the JMA scale 6-, and (b) the JMA scale 5-, during the 30 years starting from January, 2005. It reveals the fact that there is a relative high seismic hazard zone in the Tokai, Kii peninsula, and Shikoku area due to large earthquakes with a high probability of occurrence in the subduction zone of the Philippine Sea plate. Another fact also clearly shown is that surface geological condition affects seismic hazard. An area covered with soft soil such as sedimentary plains and basins has a relatively high seismic hazard.

Figure 4 shows the JMA seismic intensity corresponding to the exceedance probability of (a) 39% and (b) 5% during the 50 years starting from January 2005, respectively.

Figure 5 shows the probability that the JMA seismic intensity exceeds 6- over 30 years. The PSHM (a) considered all contributions from all earthquakes. The individual cases only considered contribution (b) from subduction zone earthquakes, (c) from major 98 faults earthquakes, and (d) from other earthquakes exclusive of cases (b) and (c).

### 3. Strong-motion evaluation for scenario earthquakes

In the National Seismic Hazard Mapping Project, both PSHMs and scenario earthquake shaking maps (SESM), which are for some earthquakes located in specified seismic faults with a high occurrence probability, are prepared. Because of the limitations of computational capacity and information on modeling, it is difficult to evaluate strong-motion using a simulation method in PSHMs. In a SESM, however, we can adopt a simulation method based on source modeling. Using the simulation method, it is possible to evaluate waveforms on an engineering bedrock layer, as well as peak acceleration and peak velocity

on ground surface. The mesh size of SESM is about 1 km. Some examples of the SESM are shown in Figure 6.

A hybrid method is adopted as the simulation method for the strong-motion evaluation. The hybrid method aims to evaluate strong-motions in a broadband frequency range. It is a combination of a deterministic approach using numerical simulation methods, such as finite difference method (FDM) or finite element method (FEM) for a low-frequency range, and a stochastic approach using the empirical or stochastic Green's function method for a high-frequency range. A lot of information on source characterization and modeling of underground structure is required for the hybrid method. Standardization of setting parameters for the hybrid method is studied in the National Seismic Hazard Mapping Project. In the following sections, we summarize technical details of the hybrid method based on the 'Recipe for strong-motion evaluation of earthquakes in active faults' and the 'Recipe for strong-motion evaluation of earthquakes in plate boundaries,' which are published by the ERCJ, (ERCJ, 2005).

#### 3.1 Setting parameters for characterized source model

Characterized source models are composed of asperities and a background slip area surrounding the asperities. Source parameters required to evaluate strong-motions using the characterized source model are classified into 3 parts. The first part is a set of outer parameters, which shows magnitude and fault shape of the earthquake. The second part is a set of parameters, which describes the degree of fault heterogeneity. The third part is a set of parameters, which defines the characteristics of rupture propagation. Details of parameters are given in the following sections and Figure 7.

##### 3.1.1 Outer parameters for characterized source model

Outer parameters of the characterized source model include location of earthquake, size of rupture area, depth, magnitude or seismic moment, and average slip on the fault.

In the National Seismic Hazard Maps, the first 3 parameters are given from the ERCJ results for a long-term evaluation of earthquake activities.

For earthquakes occurring in active fault zones, seismic moment  $M_0$  (dyne · cm) is given by referring



to the relation (ERCJ, 2005),

$$S = \begin{cases} 2.23 \cdot 10^{-15} \cdot M_0^{2/3}, & M_0 \leq 4.7 \cdot 10^{25} \\ 4.24 \cdot 10^{-11} \cdot M_0^{1/2}, & 4.7 \cdot 10^{25} < M_0 \leq 1.0 \cdot 10^{28} \end{cases} \quad (15)$$

where  $S$  ( $\text{km}^2$ ) is a rupture area estimated by the ERCJ.

For earthquakes occurring in a subduction zone or at a plate boundary, we determine the seismic moment individually by considering its characteristics for each earthquake using the seismic data set.

### 3. 1. 2 Inner parameters for characterized source model

Inner parameters for the characterized source model include locations, quantity, and areas of asperities, average slips and effective stresses inside the asperities and in the background slip area,  $f_{\max}$ , and slip velocity time function.

For earthquakes occurring in active fault zones, we determine locations of asperities by considering the investigation results for active faults, such as trench surveys, and put the asperities just under the positions where the large dislocations are observed. There are usually 1 or 2 asperities for 1 segment of an active fault. For earthquakes occurring at plate boundaries, we determine locations and quantity of asperities by considering the characteristics of each previous earthquake, using its seismic data set and results from inversion of rupture process. In this procedure, we often assume that the locations of asperities are invariants.

Using the empirical relation between seismic moments and high-frequency level of a source spectrum  $A$  ( $\text{dyne} \cdot \text{cm}/\text{s}^2$ ), the area of asperities can be given by the following relations,

$$\begin{aligned} S_a &= \pi r^2 \\ r &= \frac{7\pi}{4} \cdot \frac{M_0}{A \cdot R} \cdot \beta^2 \\ A &= 2.46 \cdot 10^{17} \cdot M_0^{1/3} \end{aligned} \quad (16)$$

where  $R$  is the radius of a circular crack whose area is the same as the fault area, and  $\beta$  is the shear wave velocity in the fault region.

The ratio of the average slip in asperities  $D_a$  and the average slip in background slip area  $D_b$  is assumed to be 2:1. The average stress drops in the asperities are given by

$$\Delta\sigma_a = \frac{7}{16} \cdot \frac{M_0}{r^2 R} \quad (17)$$

We assume that effective stress in the asperities  $\sigma_a$  is equivalent to average stress drop. The effective stress in the background domain is given by

$$\sigma_b = \frac{(D_b/W_b)}{(D_a/W_a)} \cdot \sigma_a \quad (18)$$

where  $W_a$  and  $W_b$  show width of asperity and background slip area, respectively.

We determine a cut-off frequency  $f_{\max}$  individually for each earthquake considering regional characteristics. For a slip velocity time function, we adopt a function obtained from a consideration based on the rupture simulation using a dynamic source model (Nakamura and Miyatake, 2000).

### 3. 1. 3 Other parameters for characterized source model

Other parameters for characterized source model are starting point, rupture velocities of the rupture procedure, and pattern of rupture propagation.

For earthquakes occurring in active fault zones, we can determine the starting point of the rupture using a branch pattern of the fault if there is information. The starting point then can be set up at the outer asperities. Otherwise, we put the starting point at the bottom of an asperity, if there is no information on the starting point. For earthquakes occurring at plate boundaries, we determine the starting point by considering the characteristics of each previous earthquake using its seismic data set and results of inversion of rupture process. We have assumed several cases of characteristic source models when there was not enough information, because the spatial distribution of strong-motion is strongly dependent on locations of asperities and starting point of rupture. When we have no information on rupture pattern, we assume that the rupture propagates in a concentric circle at a constant velocity from the starting point. The rupture velocity is given as follows (Geller, 1976)

$$V_r = 0.72\beta. \quad (19)$$

## 3. 2 Modeling underground structures

For the simulation, we need a seismic velocity-structure with an attenuation model to evaluate strong-motions. When modeling underground structure, we consider a deep underground structure down to the earth's crust, and/or to the plate boundary, up to the seismic bedrock ( $V_s=3$  km/s), then to the

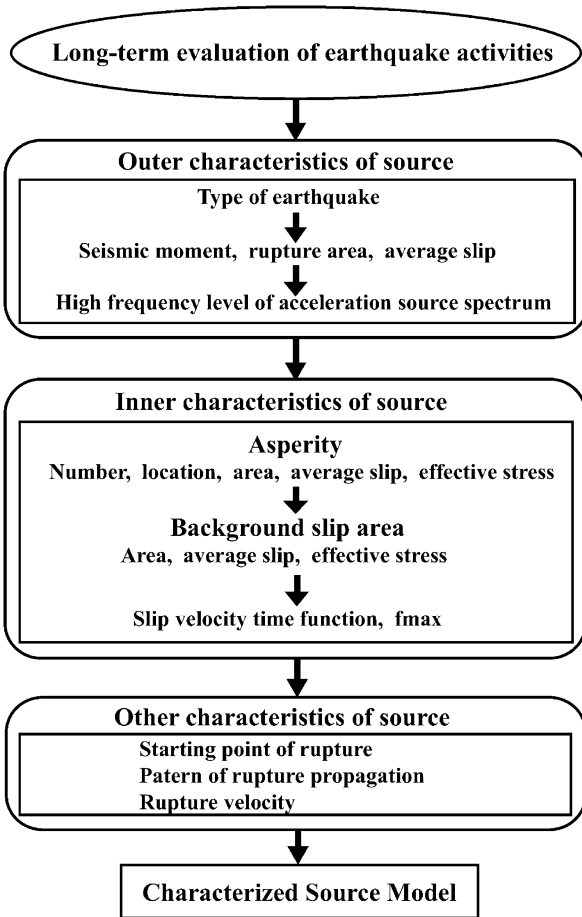


Fig. 7. Flowchart for setting source parameters.

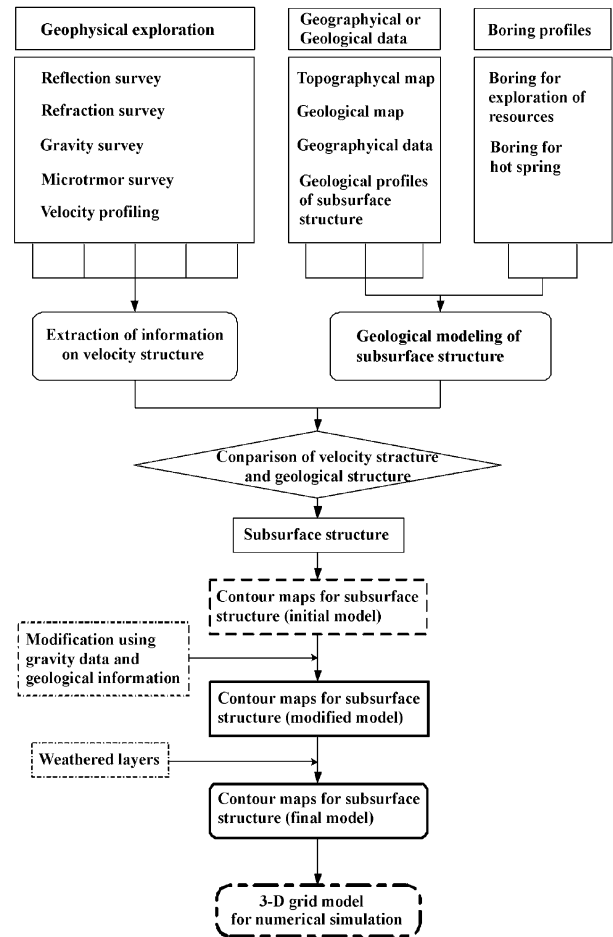


Fig. 8. Flowchart of modeling structure.

structure of an engineering bedrock layer ( $V_s=400$  m/s $\sim$ 700 m/s), and finally to the structure of surface layers as discussed below and in Figure 8.

### 3.2.1 Deep underground structure

The deep underground structure is the structure from the crust and plates up to a seismic bedrock layer with a shear velocity of 3 km/s. Using velocity and attenuation models obtained by seismic tomography or geophysical explorations, we have modeled the deep underground structure for all of Japan. A model depth down to the Moho discontinuity is required for earthquakes in active fault zones, and down to the plate boundaries for subduction earthquakes.

### 3.2.2 Structure of sediments

The structure of sediments from the seismic bedrock up to an engineering bedrock layer with a shear velocity of 400 m/s $\sim$ 700 m/s, strongly affects low-frequency strong-motions, and is an important factor for evaluating low-frequency strong-motions. When

modeling the structures of sediments, we use various profiles of deep boreholes, reflection and refraction surveys, data from microtremor surveys, as well as data from gravity surveys. We need to use an optimized modeling technique for the available data sets in a target area because quantity and quality of information on underground structure are not uniform in all areas. When modeling underground structure for strong-motion evaluations, seismic velocity structures are most important parameters. It is expected that the accuracy of modeling is proportional to the quantity and the quality of data. In an ideal case we can use all data required.

We have made a 3-dimensional structural model with various available data from throughout Japan. These include deep-borehole profiles for accurate structures at some sites, refraction profiles for boundary shapes in large sedimentary basins, reflection profiles for determining the boundary shapes of basin edges, data from microtremor surveys, gravity sur-

veys and geological information for spatial interpolation. Furthermore, we verify and modify the structural model if necessary using the above structural model to compare its simulation result of strong-motion to recorded seismograms.

In fact, however, in many cases it is difficult to obtain sufficient data from the above ideal procedure for 3-D modeling of velocity structures. In such cases, the only information distributed spatially available are data from gravity surveys and geological structure information.

Using these data, we estimate velocity structures indirectly. Uncertainty in velocity-structure modeling is increased if we use only gravity data because gravity data represent a density structure. Therefore, we also use information on geological structures to reduce uncertainty.

### 3.2.3 Structures of surface soils

When modeling the structures of surface soils from the engineering bedrock layer up to the ground surface, profiles of boreholes and surface geology data provide basic information. The surface soil structures are locally very heterogeneous, and a large amount of data is required to accurately model the surface soil structure.

If a strong-motion evaluation for a large area is required, we adopt a rough estimation method to obtain amplifications of surface soils. The rough estimation method (Fujimoto and Midorikawa, 2003) is based on Digital Nation Land Information on geological data and geomorphological data. The mesh size of these data is about 1 km. The average shear wave velocity for surface structure down to 30 m is estimated using the empirical relation between microgeographical data and the averaged shear wave velocity. Then, the amplification factors for PGV are obtained from the empirical relation between averaged shear wave velocity and PGV as shown in Figure 1.

If there is sufficient information on surface soil structures, instead of the rough method, we adopt a more accurate method by which we model the surface soil velocity-structure for each mesh using as many boring profiles and as much geological data as possible.

### 3.3 Broadband strong-motion simulation using the hybrid method

Characteristics of low-frequency strong-motions

can be explained using deterministic simulations based on physical models given by the elastodynamic theory. On the other hand, it is difficult to evaluate the characteristics of high-frequency strong-motions using deterministic approaches because the uncertainty when the setting parameters for the simulations becomes too large due to a lack of information on both source modeling and structure modeling. Instead of a deterministic approach, we need to adopt a stochastic approach to evaluate high-frequency strong-motions. Using broadband strong-motion simulations, we aim to evaluate strong-motions in the frequency range from 0.1 Hz to 10 Hz. The frequency range includes both low-frequency range and high-frequency range of strong-motions. To evaluate strong-motions in the broadband frequency range, which includes 2 frequency ranges whose physical characteristics are different, it is efficient to use a different approach to simulate strong-motions for each frequency range. Therefore, a hybrid method is proposed. The hybrid method is a combination of a deterministic approach using numerical simulation methods, such as the finite difference method (FDM) (Pitarka (1999), Aoi and Fujiwara (1999)) or the finite element method (FEM) (Fujiwara and Fujieda, 2002), to evaluate strong-motions based on theoretical models obtained from the elastodynamic theory in the low-frequency range, and a stochastic approach using the empirical or stochastic Green's function method to evaluate strong-motions in the high-frequency range. Broadband strong-motions can be obtained by superposing low-frequency strong-motions and high-frequency strong-motions using matching filters.

#### 3.3.1 Deterministic approach for simulating low-frequency strong-motions

Low-frequency strong-motions are evaluated by solving elastodynamic equations describing the seismic wave propagation for the physical model, which consists of a characteristic source model and an underground structure model. We use numerical simulation methods, e.g., FDM and FEM, to solve the equations. Rapid progress of computer technology and numerical simulation techniques enable us to solve practical problems of strong-motion evaluations. For example, in the strong-motion evaluation for earthquakes in the Morimoto-Togashi fault zone, we discretize the underground structure model of domain 90 km\*60 km\*40 km into 0.1 km meshes from the sur-



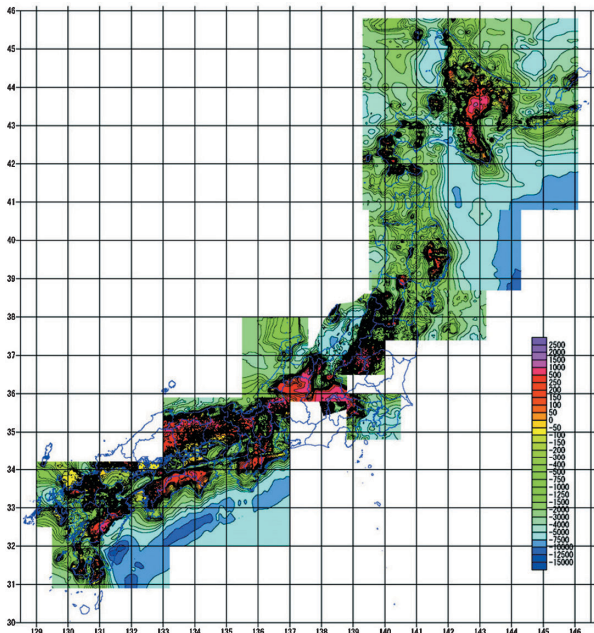


Fig. 9. Information from deep sedimentary structure model in Japan (meter).

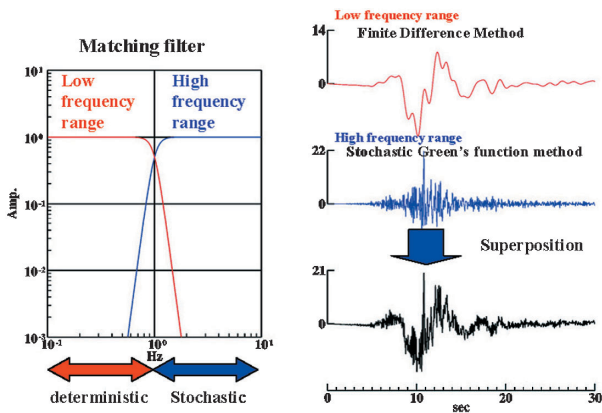


Fig. 10. The hybrid method is a combination of a deterministic approach and a stochastic approach.

face down to a depth of 4 km, and 0.3 km meshes for deeper parts. It takes 4.5 hours to calculate 6,000 time steps for this model using our FDM code in origin 3800, 64CPU. However, if we calculate using a mesh of half the size for same domain, required computation time and memory size becomes 16 times and 8 times, respectively.

### 3. 3. 2 Stochastic approach for simulating high-frequency strong-motions

We adopt the stochastic Green's function method (Dan and Sato, 1998) to evaluate high-frequency strong-motions. The stochastic Green's function method is

derived from the empirical Green's function method (Irikura (1983), Irikura (1986)). The empirical Green's function method is an evaluation method for strong-motion waveforms caused by a large earthquake using the ground motion records of earthquakes that occur in the source fault as Green's functions. The empirical Green's function method is effective for evaluating high-frequency strong-motions that are strongly affected by heterogeneities of propagation paths and local site conditions. In many cases, however, we have no ground motion record of a proper earthquake that occurred in the source fault of the target large earthquake. With the stochastic Green's function method, we use functions generated by a stochastic method instead of ground motion records for Green's functions. The stochastic Green's function method can be applied if we have no ground motion record for the Green's function. The Green's functions used in the stochastic Green's function method are stochastically approximated, and have no information on phases. The stochastic Green's function method should be used to evaluate the envelope of strong-motion waveforms.

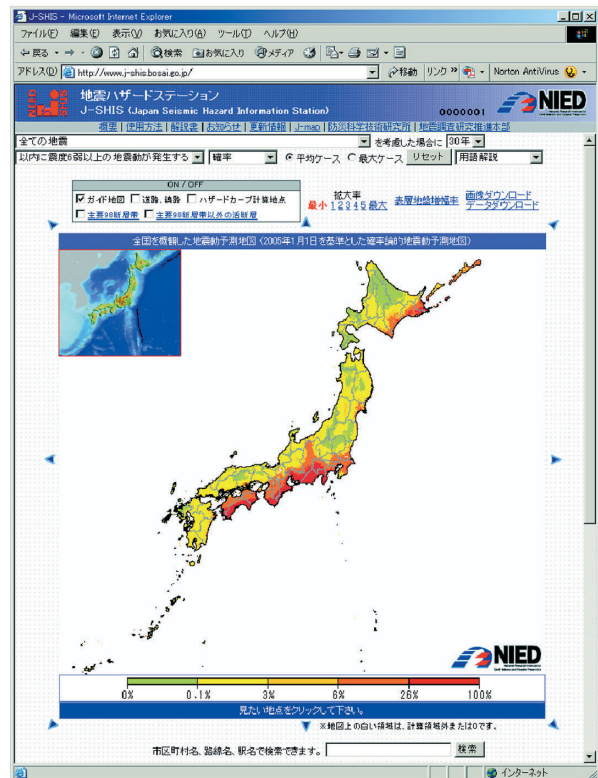


Fig. 11. Japan Seismic Hazard Information Station, J-SHIS (<http://www.j-shis.bosai.go.jp>).

### 3.3.3 The hybrid method

Using the hybrid method, we obtain broadband strong-motion waveforms by superposing low-frequency strong-motion waveforms and high-frequency strong-motion waveforms with matching filters. The matching frequency of the hybrid method usually is set lower than 1 Hz. The matching frequency should be set at a frequency in the physical transition frequency range that is between the low-frequency range, in which a deterministic approach is effective, and the high-frequency range, in which a stochastic approach is needed. Under the present circumstances, however, the matching frequency is often set at a frequency lower than the physical transition frequency range for the following three reasons:

- (L1) Limitations of computer capacity and simulation techniques,
- (L2) Limitations of modeling of rupture processes of sources,
- (L3) Limitations of information for modeling underground structures.

For reason (L1), we can expect improvements in the future because of the rapid progress of computer technology. On the other hand, we think that improvements for (L2) and (L3) require much more effort. To solve these problems, it is necessary to accumulate data obtained from seismic observation networks and surveys for underground structures, and to construct databases of them.

## 4. Relationships between 2 types of hazard map

The National Seismic Hazard Maps of Japan consists of 2 types of hazard map. One is PSHM, which shows the relation between seismic intensity value and its probability of exceedance within a certain time. The other is SESM with a specified seismic source fault. Superimposing SESMs onto probabilistic maps can be considered. The following 2 methods are proposed for the superimposition procedure.

- (M1) We make the 2 types of map independently using different techniques for strong-motion evaluations. After we complete the maps, we relate the SESMs to the probabilistic hazard maps using the contribution factor proposed by Kameda *et al.* (1997). We call this method weak superimposition.
- (M2) We make PSHMs using the hybrid method for strong-motion evaluations of all possible earthquakes. Then, each SESM evaluated using the hybrid method

is regarded as a phenomenon in the PSHMs.

In the proposed method (M1), we can select a scenario earthquake that is dominant to the strong-motion level corresponding to the probability level of interest. We can also clarify the probabilistic position of a strong-motion due to a scenario earthquake evaluated using a detailed method such as the hybrid method, by comparing the SESMs with the PSHMs or by comparing the strong-motion level directly with the seismic hazard curve at a site.

Under the present circumstances, we cannot adopt the methodology proposed in (M2) for the PSHA in the mapping project because the computation for the hybrid method is too large to carry out at present, and also because the information we currently have is not sufficient for precise source modeling and underground structure modeling. In the future, however, the methodology proposed in (M2) can be used for the PSHA to evaluate strong-motions more precisely. If we can adopt the methodology proposed in (M2), it is expected that we can directly locate a SESM as a phenomenon of the PSHM, and clarify the relationships between the 2 types of hazard map.

## 5. Japan Seismic Hazard Information Station, J-SHIS

We developed an open web system to provide information interactively and retrievably for the hazard maps. We named this system Japan Seismic Hazard Information Station, J-SHIS (<http://www.jshis.bosai.go.jp>). We aimed to disseminate processes of uncertainty evaluation, and to meet multi-purpose needs in engineering fields. The information provided by J-SHIS includes not only the results of the hazard maps, but also various information required in the processes of making the hazard maps, such as data on seismic activity, source models, and underground structure. We will develop and maintain the J-SHIS as seismic hazard information sharing bases.

## 6. Discussion

The reliability of an intensity level with a small probability of an earthquake, whose occurrence probability is high, becomes a subject of discussion in the preparation of PSHMs. An intensity level with a small probability is sometimes strongly affected by the amount of uncertainty contained in an empirical attenuation relation used in a seismic hazard analy-

sis. We often adopt a deviation value, which is obtained from statistical regression analyses, to derive the attenuation relation. However, it consists of uncertainties from various sources because the empirical attenuation relation is based on data observed at various sites from various earthquakes. It has been pointed out that this procedure overestimates a seismic hazard because a spatial uncertainty is to be considered separately as an epistemic uncertainty. On the other hand, if we use a stochastic Green's function method or a hybrid method, instead of the empirical attenuation relation in the strong-motion evaluation, the spatial uncertainty is not combined, and the result is more realistic. Further studies from both data and theory are necessary to properly quantify the uncertainty in a ground motion evaluation.

A Brownian passage time distribution and a Poisson process are adopted for a long-term evaluation of earthquake activity by ERCJ. Because of insufficient information on previous earthquake activity in fault zones, the average recurrence interval and elapsed time since the latest earthquake event are often expressed as a time range instead of a fixed value. Consequently, the occurrence probability is given by an interval. In PSHMs, based on a discussion on the treatment of the probability given by an interval, we adopt the median for a typical case, and the maximum probability value for reference.

Although not only estimated parameters but also degrees of reliability of estimations of parameters are shown in a long-term evaluation of earthquake activity, it is quite difficult to quantify degrees of reliability, so they are not reflected in the hazard maps.

It is essential to select a specified earthquake to make a SESM. The basic policy for selecting a scenario earthquake in the National Seismic Hazard Mapping Project is to choose the most probable case. However, available information to determine the source parameters of the scenario earthquake is often insufficient, and a decision under a situation in which uncertain factors are present is required. When we do not have sufficient information, we assume several cases of characteristic source model, and compare the results to show the deviations among strong-motion evaluations due to uncertainties. This is still under consideration because there remain problems to be solved when evaluating the reliability of

results under a situation with uncertainty.

To improve the accuracy of the hybrid method, it is indispensable to expand computer capacity and develop simulation techniques, while improving rupture processes of source modeling and modeling of underground structures. We can expect developments related to computer capacity and simulation techniques in the future because of the rapid progress of computer technology. On the other hand, many more improvements are required in the rupture processes of source modeling and for modeling of underground structures. The long-term policy should be to promote the gathering of data obtained from seismic observation networks and surveys for underground structures, and to construct related databases.

A 1-kilometer mesh is used at present because PSHM discussed a concept map for all of Japan. Obviously, a precise map is required for disaster mitigation by the public and municipalities. This is under study, and our target is to achieve it in the next five years.

#### Acknowledgments

This study was done under the direction of the ERCJ (Chairman: Kenshiro Tsumura), the subcommittee for long-term evaluations (Chairman: Kunihiko Shimazaki) and the subcommittee for evaluations of strong ground motion (Chairman: Kojiro Irikura). We are deeply grateful for valuable comments from the committee for methodology of PSHA (Chairman: Saburo Midorikawa) and the committee for using seismic hazard maps (Chairman: Hiroyuki Kameda). Dr. K.X. Hao kindly read our manuscript. His comments were useful to improve this paper.

#### References

- Aoi S and Fujiwara H. (1999), 3D finite-difference method using discontinuous grids. *Bull. Seism. Soc. Amer.*, 89, 918–930.
- Dan K and Sato T. (1998), Strong-motion prediction by semi-empirical method based on variable-slip rupture model of earthquake fault. (in Japanese) *J. Struct. Constr. Eng.*, AIJ, 509, 49–60.
- Earthquake research committee of Japan (2005), General seismic hazard map covering whole of Japan, (in Japanese).
- Fujimoto K and Midorikawa S. (2003), Average shear-wave mapping throughout Japan using the Digital National Land information. (in Japanese) *Journal of JAEE*, 3, 13–27.

- Fujiwara H and Fujieda T. (2002), Voxel finite element method for 3-D elastodynamic analysis. (in Japanese) Proceedings of the 11th Japan Earthquake Engineering Symposium, 94.
- Geller R.J. (1976) Scaling relations for earthquake source parameters and magnitudes. *Bull. Seism. Soc. Amer.*, 66, 1501–1523.
- Irikura K. (1983), Semi-empirical estimation of strong ground motions during large earthquakes. *Bulletin of the Disaster Prevention Research Institute, Kyoto University*, Vol. 33, Part 2, No. 298, 63–104.
- Irikura K. (1986), Prediction of strong acceleration motions using empirical Green's function. Proceedings of the Seventh Japan Earthquake Engineering Symposium, 151–156.
- Kameda H, Ishikawa Y, Okumura T and Nakajima M. (1997), Probabilistic scenario earthquakes -definition and engineering applications-. (in Japanese) *Journal of Structural Mechanics and Earthquake Engineering, JSCE*, 577, 75–87.
- Midorikawa S, Fujimoto K, Muramatsu I. (1999), Correlation of new J.M.A. instrumental seismic intensity with former J.M.A. seismic intensity and ground motion parameters. (in Japanese) *Journal of ISSS*, 1, 51–56.
- Nakamura H and Miyatake T. (2000), An approximate expression of slip velocity time function for simulation of near-field strong ground motion. (in Japanese) *Zisin*, 53, 1–9.
- Pitarka A. (1999), 3D elastic finite-difference modeling of seismic motion using staggered grids with non-uniform spacing. *Bull. Seism. Soc. Amer.*, 89, 54–68.
- Si H, and Midorikawa S. (1999), New attenuation relationships for peak ground acceleration and velocity considering effects of fault type and site condition. (in Japanese) *J. Struct. Constr. Eng., AIJ*, 523, 63–70.

(Received December 23, 2005)

(Accepted July 5, 2006)